

Search for Lepton-Flavor-Violating τ Decays into a Lepton and a Vector Meson

Y. Miyazaki,²⁷ H. Aihara,⁴⁸ K. Arinstein,^{1,36} V. Aulchenko,^{1,36} A. M. Bakich,⁴²
V. Balagura,¹⁵ E. Barberio,²⁶ A. Bay,²² K. Belous,¹³ V. Bhardwaj,³⁸ M. Bischofberger,²⁸
A. Bondar,^{1,36} A. Bozek,³² M. Bračko,^{24,16} T. E. Browder,⁸ A. Chen,²⁹ P. Chen,³¹
B. G. Cheon,⁷ C.-C. Chiang,³¹ I.-S. Cho,⁵² K. Cho,¹⁹ K.-S. Choi,⁵² Y. Choi,⁴¹
J. Dalseno,^{25,44} M. Danilov,¹⁵ Z. Doležal,² A. Drutskoy,⁴ S. Eidelman,^{1,36} D. Epifanov,^{1,36}
N. Gabyshev,^{1,36} A. Garmash,^{1,36} B. Golob,^{23,16} H. Ha,²⁰ J. Haba,⁹ K. Hara,²⁷
K. Hayasaka,²⁷ H. Hayashii,²⁸ Y. Horii,⁴⁷ Y. Hoshi,⁴⁶ W.-S. Hou,³¹ Y. B. Hsiung,³¹
H. J. Hyun,²¹ T. Iijima,²⁷ K. Inami,²⁷ R. Itoh,⁹ M. Iwabuchi,⁵² N. J. Joshi,⁴³ T. Julius,²⁶
D. H. Kah,²¹ J. H. Kang,⁵² H. Kawai,³ T. Kawasaki,³⁴ C. Kiesling,²⁵ H. J. Kim,²¹
H. O. Kim,²¹ M. J. Kim,²¹ Y. J. Kim,⁶ K. Kinoshita,⁴ B. R. Ko,²⁰ P. Križan,^{23,16}
T. Kumita,⁴⁹ A. Kuzmin,^{1,36} Y.-J. Kwon,⁵² S.-H. Kyeong,⁵² J. S. Lange,⁵ M. J. Lee,⁴⁰
S.-H. Lee,²⁰ Y. Li,⁵¹ C. Liu,³⁹ Y. Liu,³¹ D. Liventsev,¹⁵ R. Louvot,²² S. McOnie,⁴²
K. Miyabayashi,²⁸ H. Miyata,³⁴ R. Mizuk,¹⁵ G. B. Mohanty,⁴³ A. Moll,^{25,44} T. Mori,²⁷
Y. Nagasaka,¹⁰ E. Nakano,³⁷ M. Nakao,⁹ H. Nakazawa,²⁹ Z. Natkaniec,³² S. Nishida,⁹
O. Nitoh,⁵⁰ S. Ogawa,⁴⁵ T. Ohshima,²⁷ S. Okuno,¹⁷ G. Pakhlova,¹⁵ C. W. Park,⁴¹
H. Park,²¹ H. K. Park,²¹ R. Pestotnik,¹⁶ M. Petrič,¹⁶ L. E. Pilonen,⁵¹ A. Poluektov,^{1,36}
M. Röhrken,¹⁸ S. Ryu,⁴⁰ H. Sahoo,⁸ K. Sakai,⁹ Y. Sakai,⁹ O. Schneider,²² C. Schwanda,¹⁴
K. Senyo,²⁷ M. E. Sevier,²⁶ M. Shapkin,¹³ V. Shebalin,^{1,36} C. P. Shen,⁸ J.-G. Shiu,³¹
B. Shwartz,^{1,36} F. Simon,^{25,44} P. Smerkol,¹⁶ Y.-S. Sohn,⁵² A. Sokolov,¹³ S. Stanič,³⁵
M. Starič,¹⁶ T. Sumiyoshi,⁴⁹ Y. Teramoto,³⁷ K. Trabelsi,⁹ S. Uehara,⁹ T. Uglov,¹⁵
Y. Unno,⁷ S. Uno,⁹ Y. Usov,^{1,36} S. E. Vahsen,⁸ G. Varner,⁸ A. Vinokurova,^{1,36}
A. Vossen,¹¹ C. H. Wang,³⁰ P. Wang,¹² M. Watanabe,³⁴ Y. Watanabe,¹⁷
K. M. Williams,⁵¹ E. Won,²⁰ H. Yamamoto,⁴⁷ Y. Yamashita,³³ Z. P. Zhang,³⁹
V. Zhilich,^{1,36} V. Zhulanov,^{1,36} T. Zivko,¹⁶ A. Zupanc,¹⁸ and O. Zyukova^{1,36}

(The Belle Collaboration)

¹*Budker Institute of Nuclear Physics, Novosibirsk, Russian Federation*

²*Faculty of Mathematics and Physics,*

Charles University, Prague, The Czech Republic

³*Chiba University, Chiba, Japan*

⁴*University of Cincinnati, Cincinnati, OH, USA*

⁵*Justus-Liebig-Universität Gießen, Gießen, Germany*

⁶*The Graduate University for Advanced Studies, Hayama, Japan*

⁷*Hanyang University, Seoul, South Korea*

⁸*University of Hawaii, Honolulu, HI, USA*

⁹*High Energy Accelerator Research Organization (KEK), Tsukuba, Japan*

- ¹⁰*Hiroshima Institute of Technology, Hiroshima, Japan*
- ¹¹*University of Illinois at Urbana-Champaign, Urbana, IL, USA*
- ¹²*Institute of High Energy Physics,
Chinese Academy of Sciences, Beijing, PR China*
- ¹³*Institute for High Energy Physics, Protvino, Russian Federation*
- ¹⁴*Institute of High Energy Physics, Vienna, Austria*
- ¹⁵*Institute for Theoretical and Experimental Physics, Moscow, Russian Federation*
- ¹⁶*J. Stefan Institute, Ljubljana, Slovenia*
- ¹⁷*Kanagawa University, Yokohama, Japan*
- ¹⁸*Institut für Experimentelle Kernphysik,
Karlsruher Institut für Technologie, Karlsruhe, Germany*
- ¹⁹*Korea Institute of Science and Technology Information, Daejeon, South Korea*
- ²⁰*Korea University, Seoul, South Korea*
- ²¹*Kyungpook National University, Taegu, South Korea*
- ²²*École Polytechnique Fédérale de Lausanne, EPFL, Lausanne, Switzerland*
- ²³*Faculty of Mathematics and Physics,
University of Ljubljana, Ljubljana, Slovenia*
- ²⁴*University of Maribor, Maribor, Slovenia*
- ²⁵*Max-Planck-Institut für Physik, München, Germany*
- ²⁶*University of Melbourne, Victoria, Australia*
- ²⁷*Nagoya University, Nagoya, Japan*
- ²⁸*Nara Women's University, Nara, Japan*
- ²⁹*National Central University, Chung-li, Taiwan*
- ³⁰*National United University, Miao Li, Taiwan*
- ³¹*Department of Physics, National Taiwan University, Taipei, Taiwan*
- ³²*H. Niewodniczanski Institute of Nuclear Physics, Krakow, Poland*
- ³³*Nippon Dental University, Niigata, Japan*
- ³⁴*Niigata University, Niigata, Japan*
- ³⁵*University of Nova Gorica, Nova Gorica, Slovenia*
- ³⁶*Novosibirsk State University, Novosibirsk, Russian Federation*
- ³⁷*Osaka City University, Osaka, Japan*
- ³⁸*Panjab University, Chandigarh, India*
- ³⁹*University of Science and Technology of China, Hefei, PR China*
- ⁴⁰*Seoul National University, Seoul, South Korea*
- ⁴¹*Sungkyunkwan University, Suwon, South Korea*
- ⁴²*School of Physics, University of Sydney, NSW 2006, Australia*
- ⁴³*Tata Institute of Fundamental Research, Mumbai, India*
- ⁴⁴*Excellence Cluster Universe, Technische Universität München, Garching, Germany*
- ⁴⁵*Toho University, Funabashi, Japan*
- ⁴⁶*Tohoku Gakuin University, Tagajo, Japan*
- ⁴⁷*Tohoku University, Sendai, Japan*
- ⁴⁸*Department of Physics, University of Tokyo, Tokyo, Japan*
- ⁴⁹*Tokyo Metropolitan University, Tokyo, Japan*
- ⁵⁰*Tokyo University of Agriculture and Technology, Tokyo, Japan*
- ⁵¹*CNP, Virginia Polytechnic Institute and State University, Blacksburg, VA, USA*
- ⁵²*Yonsei University, Seoul, South Korea*

Abstract

We search for lepton-flavor-violating $\tau \rightarrow \ell V^0$ decays, where ℓ is an electron or muon and V^0 is one of the vector mesons ρ^0 , ϕ , ω , K^{*0} and \bar{K}^{*0} . We use 854 fb^{-1} of data collected with the Belle detector at the KEKB asymmetric-energy e^+e^- collider. No evidence for a signal is found in any decay mode, and we obtain 90% confidence level upper limits on the individual branching fractions in the range $(1.2 - 8.4) \times 10^{-8}$.

PACS numbers: 11.30.Fs; 13.35.Dx; 14.60.Fg

INTRODUCTION

Lepton flavor violation (LFV) in charged lepton decays is forbidden in the Standard Model (SM) and remains highly suppressed even if the SM is modified to include neutrino mixing. However, extensions of the SM, such as supersymmetry, leptoquark and many other models [1–7] predict LFV with branching fractions as high as 10^{-8} , which could already be accessible in current B -factory experiments. We search for $\tau^- \rightarrow \ell^- V^0$ decays[†], where ℓ is an electron or muon and V^0 is one of the vector mesons ρ^0 , ϕ , ω , K^{*0} or \bar{K}^{*0} . These results are based on the entire 854 fb^{-1} data sample collected at center-of-mass (CM) energies near the $\Upsilon(4S)$, near the $\Upsilon(5S)$, and off resonance with the Belle detector [8] at the KEKB asymmetric-energy e^+e^- collider [9]. Previously, we obtained 90% confidence level (C.L.) upper limits on branching fractions of these decays using 543 fb^{-1} of data; the results were in the range $(5.8\text{--}18) \times 10^{-8}$ [10]. The results described here use additional data and an improved event selection procedure, which is optimized mode-by-mode. The BaBar collaboration has also published 90% C.L. upper limits in the range $(2.6\text{--}19) \times 10^{-8}$ using 451 fb^{-1} of data [11] for all $\tau^- \rightarrow \ell^- V^0$ decays except for $\tau^- \rightarrow \ell^- \omega$ for which 384 fb^{-1} of data were used [12].

The Belle detector is a large-solid-angle magnetic spectrometer that consists of a silicon vertex detector (SVD), a 50-layer central drift chamber (CDC), an array of aerogel threshold Cherenkov counters (ACC), a barrel-like arrangement of time-of-flight scintillation counters (TOF), and an electromagnetic calorimeter comprised of CsI(Tl) crystals (ECL), all located inside a superconducting solenoid coil that provides a 1.5 T magnetic field. An iron flux-return located outside of the coil is instrumented to detect K_L^0 mesons and to identify muons (KLM). The detector is described in detail elsewhere [8].

Particle identification is very important for this measurement. We use particle identification likelihood variables based on the ratio of the energy deposited in the ECL to the momentum measured in the SVD and CDC, shower shape in the ECL, the particle’s range in the KLM, hit information from the ACC, dE/dx measured in the CDC, and the particle’s time of flight. To distinguish hadron species, we use likelihood ratios, $\mathcal{P}(i/j) = \mathcal{L}_i/(\mathcal{L}_i + \mathcal{L}_j)$, where \mathcal{L}_i (\mathcal{L}_j) is the likelihood of the observed detector response for a track with flavor i (j). For lepton identification, we form likelihood ratios $\mathcal{P}(e)$ [13] and $\mathcal{P}(\mu)$ [14] using the responses of the appropriate subdetectors.

We use Monte Carlo (MC) samples to estimate the signal efficiency and optimize the event selection. Signal and background events from generic $\tau^+\tau^-$ decays are generated by KKMC/TAUOLA [15]. For signal, we generate $e^+e^- \rightarrow \tau^+\tau^-$ events, in which one τ is forced to decay into a lepton and a vector meson using a two-body phase space model, while the other τ decays generically. Background events $B\bar{B}$, continuum $e^+e^- \rightarrow q\bar{q}$ ($q = u, d, s, c$), Bhabha, and two-photon processes are generated by EvtGen [16], BHLUMI [17], and AAFH [18], respectively. In what follows, all kinematic variables are calculated in the laboratory frame unless otherwise specified. In particular, variables calculated in the e^+e^- CM frame are indicated by the superscript “CM”.

[†] Throughout this paper, charge-conjugate modes are implied unless stated otherwise.

TABLE I: Allowed ranges for the mass of V^0 candidates and for the cosine of the angle between the missing particle and the tag-side track in the CM system ($\cos \theta_{\text{tag-miss}}^{\text{CM}}$).

V^0	Invariant mass (GeV/c^2)	$\cos \theta_{\text{tag-miss}}^{\text{CM}}$ for $\tau \rightarrow \mu V^0$ (eV^0)
ρ^0	$0.587 < M_{\pi\pi} < 0.962$	$[0.0, 0.85]$ ($[0.0, 0.96]$)
ϕ	$1.009 < M_{KK} < 1.031$	$[0.0, 0.88]$ ($[0.0, 0.97]$)
ω	$0.757 < M_{\pi\pi\pi} < 0.808$	$[0.0, 0.88]$ ($[0.0, 0.97]$)
$K^{*0}(\bar{K}^{*0})$	$0.842 < M_{K\pi} < 0.956$	$[0.0, 0.87]$ ($[0.0, 0.96]$)

EVENT SELECTION

We search for $e^+e^- \rightarrow \tau^+\tau^-$ events in which one τ (the signal τ) decays into a lepton and a vector meson ($V^0 = \rho^0, \phi, \omega, K^{*0}$ and \bar{K}^{*0}) and the other τ (the tag τ) results in a single charged track, any number of additional photons, and neutrinos. We reconstruct ρ^0 from $\pi^+\pi^-$, ϕ from K^+K^- , ω from $\pi^+\pi^-\pi^0$, K^{*0} from $K^+\pi^-$ and \bar{K}^{*0} from $K^-\pi^+$. To improve sensitivity compared to our previous work [10], the event selection is optimized mode-by-mode, since the backgrounds are mode dependent.

For each candidate event we calculate the ℓV^0 invariant mass ($M_{\ell V^0}$) and the difference of the ℓV^0 energy from the beam energy in the CM frame (ΔE). In the two-dimensional distribution of $M_{\ell V^0}$ versus ΔE , signal events should have $M_{\ell V^0}$ close to the τ -lepton mass (m_τ) and ΔE close to zero.

We require that events contain four charged tracks and any number of photons within the fiducial volume defined by $-0.866 < \cos \theta < 0.956$, where θ is the polar angle relative to the direction opposite to that of the incident e^+ beam in the laboratory frame. The transverse momentum (p_t) of each charged track and the energy of each photon (E_γ) are required to satisfy $p_t > 0.1 \text{ GeV}/c$ and $E_\gamma > 0.1 \text{ GeV}$, respectively. For each charged track, the distance of the closest point with respect to the interaction point is required to be less than 0.5 cm in the transverse direction and less than 3.0 cm in the longitudinal direction.

Using the plane perpendicular to the CM thrust axis [19], which is calculated from the observed tracks and photon candidates, we separate the particles in an event into two hemispheres. These are referred to as the signal and tag sides. The tag side is required to contain one charged track while the signal side is required to contain three charged tracks. We require one charged track on the signal side to be identified as a lepton. Electron candidates are required to have $\mathcal{P}(e) > 0.9$ and momenta $p > 0.6 \text{ GeV}/c$ while muon candidates should have $\mathcal{P}(\mu) > 0.95$ and $p > 1.0 \text{ GeV}/c$. In order to take into account the emission of bremsstrahlung photons from electrons, the momentum of the electron track is reconstructed by adding to it the momentum of every photon within 0.05 radians of the track direction. With these requirements, the electron (muon) identification efficiency is 91% (85%) while the probability to misidentify a pion as an electron (a muon) is below 0.5% (2%).

Charged kaons are identified by the condition $\mathcal{P}(K/\pi) > 0.8$ for the $\tau \rightarrow \ell K^{*0}$ and $\ell \bar{K}^{*0}$ modes (> 0.6 for the $\ell \phi$ modes). Charged pions must satisfy the requirement $\mathcal{P}(K/\pi) < 0.6$ for the $\tau \rightarrow \ell \rho^0, \ell K^{*0}$ and $\ell \bar{K}^{*0}$ modes. We do not require charged pion identification for the $\tau \rightarrow \ell \omega$ modes. The kaon (pion) identification efficiency is 80% (88%) while the probability to misidentify a pion (kaon) as a kaon (a pion) is below 10% (12%). In order to reduce the fake vector meson background from photon conversions (i.e., $\gamma \rightarrow e^+e^-$), we require that the two charged tracks from the meson candidate have $\mathcal{P}(e) < 0.1$. Furthermore, we require

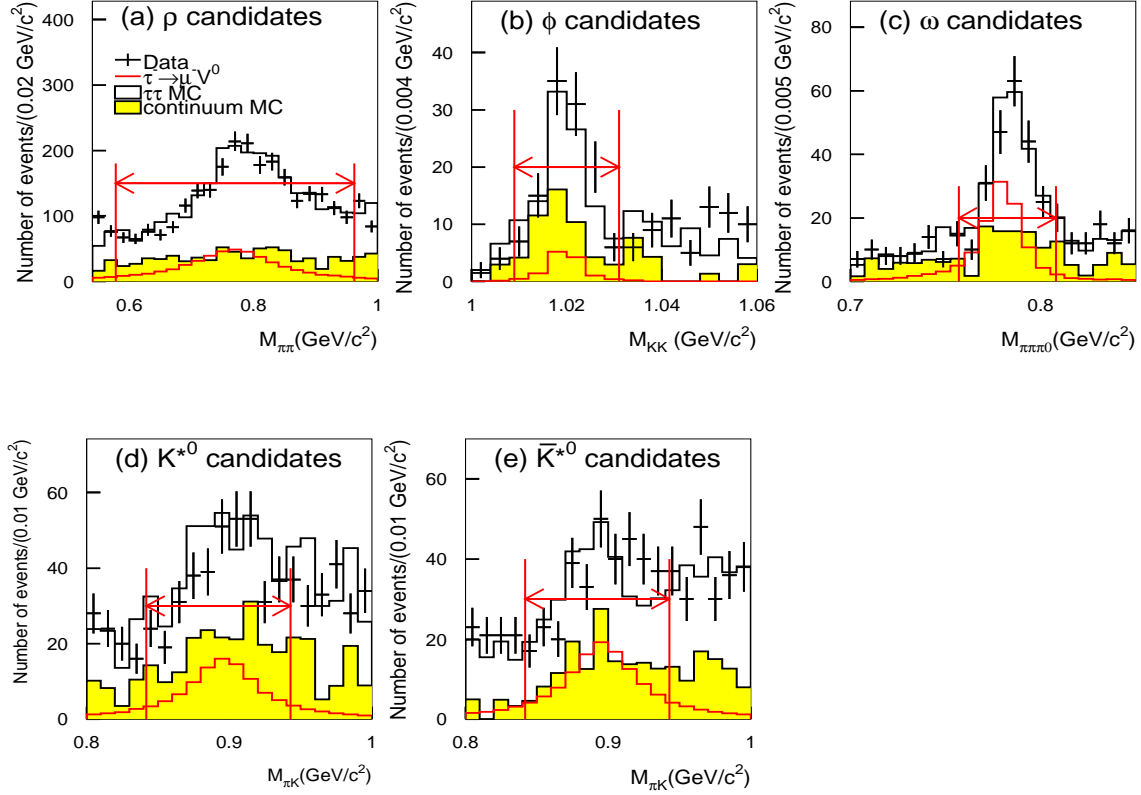


FIG. 1: Vector meson invariant mass distributions for the $\tau \rightarrow \mu V^0$ modes after the baseline selection (before vector meson mass requirements) in the region $1.5 \text{ GeV}/c^2 < M_{\ell V^0} < 2.0 \text{ GeV}/c^2$ and $-0.5 \text{ GeV} < \Delta E < 0.5 \text{ GeV}$: (a), (b), (c), (d) and (e) show the $\tau \rightarrow \mu \rho^0$, $\mu \phi$, $\mu \omega$, μK^{*0} and $\mu \bar{K}^{*0}$ modes, respectively. The signal MC ($\tau \rightarrow \mu V^0$) distributions are normalized arbitrarily while the background MC distributions are normalized to the data luminosity. Selected mass regions are indicated by arrows.

$\mathcal{P}(\mu) < 0.1$ to suppress $e^+e^- \rightarrow e^+e^-\mu^+\mu^-$ two-photon background. For the $\tau \rightarrow \ell \omega$ modes, we select $\pi^0(\rightarrow \gamma\gamma)$ candidates on the signal side by requiring $E_\gamma > 0.1 \text{ GeV}$ and $p_{\pi^0} > 0.4 \text{ GeV}/c$, which suppresses incorrectly reconstructed π^0 candidates from initial-state radiation (ISR) and beam background. The π^0 mass window is $0.12 \text{ GeV}/c^2 < M_{\gamma\gamma} < 0.15 \text{ GeV}/c^2$.

To ensure that the missing particles are neutrinos rather than photons or charged particles that pass outside the detector acceptance, we impose requirements on the missing momentum \vec{p}_{miss} , which is calculated by subtracting the vector sum of the momenta of all tracks and photons from the sum of the e^+ and e^- beam momenta. We require that $|p_{\text{miss}}^t|$, the magnitude of the transverse component of \vec{p}_{miss} , be greater than $0.5 \text{ GeV}/c$ ($0.7 \text{ GeV}/c$) for the $\tau \rightarrow \mu V^0$ (eV^0 except the $e\rho^0$) modes, and that \vec{p}_{miss} point into the fiducial volume of the detector. For the $\tau \rightarrow e\rho^0$ mode only, we apply the more restrictive selection requirement $|p_{\text{miss}}^t| > 1.5 \text{ GeV}/c$. Furthermore, we reject events if the direction of the missing momentum traverses the gap between the barrel and the endcap since an undetected photon may be incorrectly attributed to missing particles.

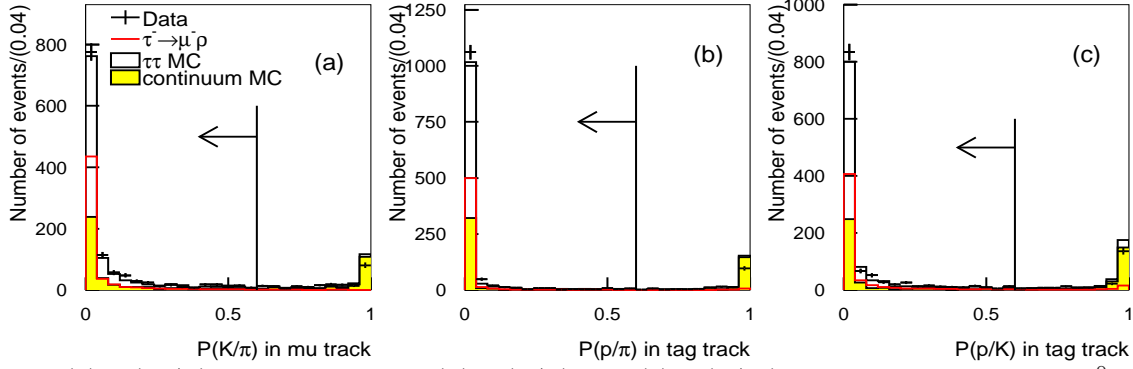


FIG. 2: (a) $\mathcal{P}(K/\pi)$ for muon tracks, (b) $\mathcal{P}(p/\pi)$ and (c) $\mathcal{P}(p/K)$ for hadronic tags, for $\mu\rho^0$ candidate events satisfying $1.5 \text{ GeV}/c^2 < M_{\ell V^0} < 2.0 \text{ GeV}/c^2$ and $-0.5 \text{ GeV} < \Delta E < 0.5 \text{ GeV}$. Signal MC ($\tau \rightarrow \mu\rho^0$) distributions are normalized arbitrarily while the background MC distributions are normalized to the data luminosity. Selected regions are indicated by arrows.

To suppress $B\bar{B}$ and $q\bar{q}$ background, we require that the number of photons on the tag side, n_{γ}^{TAG} , satisfy $n_{\gamma}^{\text{TAG}} \leq 2$ (≤ 1) for hadronic (leptonic) tags. For all modes except $\pi^0 \rightarrow \gamma\gamma$, we also require at most one photon on the signal side.

We select vector mesons whose invariant mass satisfies the requirements shown in Table I and Fig. 1. MC simulation predicts that for the $\tau \rightarrow \mu V^0$ modes the dominant background comes from continuum and generic $\tau^+\tau^-$ -events, whereas for the $\tau \rightarrow e V^0$ modes it originates from inelastic V^0 -photoproduction ($e^+e^- \rightarrow e^+e^-V^0$) and two-photon processes.

Since neutrinos are emitted on the tag side only, the direction of \vec{p}_{miss} should lie within the tag side of the event. The cosine of the opening angle between \vec{p}_{miss} and the charged track on the tag side in the CM system, $\cos\theta_{\text{tag-miss}}^{\text{CM}}$, is required to be greater than zero. If the track on the tag side is a hadron, then for the $\tau \rightarrow \mu V^0$ modes we also require $\cos\theta_{\text{tag-miss}}^{\text{CM}} < (0.85 - 0.88)$. This $\cos\theta_{\text{tag-miss}}^{\text{CM}}$ requirement reduces continuum background with missing energy due to neutrons or K_L 's since the masses of the neutron and K_L are higher than that of the neutrino. We also require that $\cos\theta_{\text{tag-miss}}^{\text{CM}} < (0.96 - 0.97)$ for the $\tau \rightarrow e V^0$ modes. This requirement can reduce Bhabha, inelastic V^0 -photoproduction, and two-photon background, since radiated photons from the tag-side track result in missing momentum if they overlap with the ECL clusters associated with the tag-side track [20]. The $\cos\theta^{\text{CM}}$ requirements for all modes are given in Table I.

For the $\tau \rightarrow \mu V^0$ modes, a muon can originate from a kaon decaying in the CDC ($K^\pm \rightarrow \mu^\pm \nu_\mu$). Therefore, we apply a kaon veto, $\mathcal{P}(K/\pi) < 0.6$, for muon candidate tracks if the tag side track is a hadron (see Fig. 2 (a)). Another important continuum background predicted by MC is from dibaryon production with a proton on the tag side. Therefore, we apply a proton veto, $\mathcal{P}(p/\pi) < 0.6$ and $\mathcal{P}(p/K) < 0.6$, as shown in Figs. 2 (b) and (c). To reject $q\bar{q}$ continuum background, we require that the magnitude of thrust (T) be greater than 0.90. The reconstructed mass of the charged track and photons on the tag side, m_{tag} , is required to be less than the τ lepton mass ($1.777 \text{ GeV}/c^2$). To reduce $e^+e^- \rightarrow \mu^+\mu^-$ background for the $\tau \rightarrow \mu\rho^0$ mode only, we also require that the momentum of the track on the tag side in the CM system be less than $4.0 \text{ GeV}/c$ if the track is a muon candidate.

For the $\tau \rightarrow e V^0$ modes, photon conversions can result in large backgrounds when an e^+e^- pair is incorrectly reconstructed as a fake vector meson. Fake vector mesons can also originate from one of the electrons in a photon conversion and a hadron. As seen from

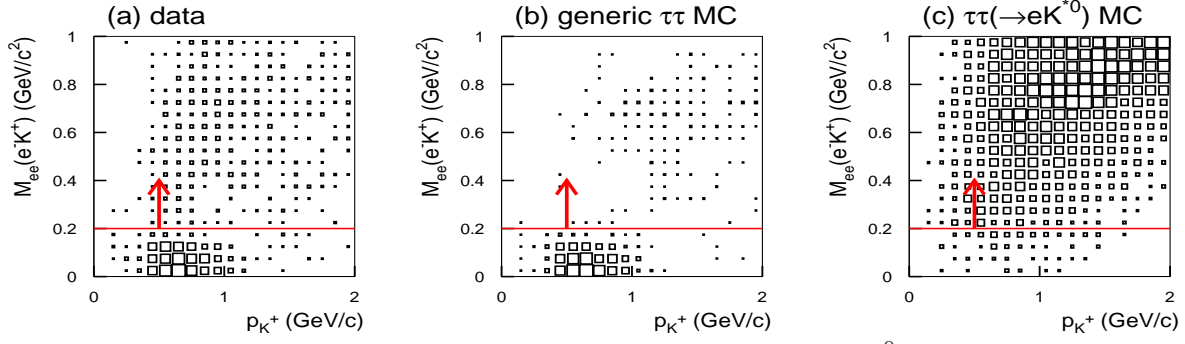


FIG. 3: Scatter-plot of the momentum of kaon candidates from K^{*0} candidates, p_{K^+} , versus the invariant mass of electron and kaon candidates from $\tau \rightarrow eK^{*0}(\rightarrow K^+\pi^-)$ reconstructed by assigning the electron mass to the kaon tracks, $M_{ee}(e^-K^+)$, for the eK^{*0} mode: (a), (b) and (c) show the distributions for data, generic $\tau\tau$ MC and $\tau\tau(\rightarrow eK^{*0})$ MC, respectively. Selected regions are indicated by red lines and arrows.

generic $\tau^+\tau^-$ MC, such a background comes from $\tau^- \rightarrow h^-\pi^0(\rightarrow \gamma\gamma)\nu_\tau$ decays. When a γ from the π^0 -decay converts and one of the conversion electrons traverses the ECL gap, then it may incorrectly be classified as a hadron because the electron veto does not work. In the momentum range between 0.5 GeV/c and 1.0 GeV/c such an electron can be misidentified as a kaon because the dE/dx distributions of kaons and electrons overlap. In other momentum ranges the electron can be misidentified as a pion. If we assign an electron mass to such a fake hadron, then the invariant mass $M_{ee}(e^-h^+)$ will be small, as expected for conversions. Therefore we require $M_{ee}(e^-h^+)(M_{ee}(h^-h^+)) > 0.2 \text{ GeV}/c^2$ for e^-h^+ (h^-h^+) candidates for the $e\rho^0$, eK^{*0} and $e\bar{K}^{*0}$ modes. Background from such e^-K^+ events in the eK^{*0} mode is shown in Fig. 3. For the $\tau \rightarrow e\rho^0$ mode only we also require that the magnitude of the thrust be in the range $0.90 < T < 0.96$ to reduce two-photon and inelastic V^0 -production backgrounds.

SIGNAL AND BACKGROUND ESTIMATION

For all modes, the $M_{\ell V^0}$ and ΔE resolutions are obtained from fits to the signal MC distributions, using an asymmetric Gaussian function that takes into account initial-state radiation. These Gaussians have widths as shown in Table II.

To evaluate branching fractions, we use elliptical signal regions with major and minor axes equal to 3σ in the ΔE and $M_{\ell V^0}$ distributions, where $\sigma = (\sigma^{\text{high}} + \sigma^{\text{low}})/2$ from Table II. The center and rotation angle are determined by scanning to maximize the efficiency of the signal divided by the area. We blind the data in the signal region until all selection criteria are finalized so as not to bias our choice of selection criteria.

Figures 4 and 5 show scatter-plots for data events and signal MC samples distributed over $\pm 20\sigma$ in the $M_{\ell V^0} - \Delta E$ plane for the $\tau \rightarrow \mu V^0$ and $e V^0$ modes, respectively. For the $\tau \rightarrow e V^0$ modes, the dominant background comes from two-photon processes, while the fraction of $q\bar{q}$ and generic $\tau^+\tau^-$ events is small due to the low electron fake rate. For the $\tau \rightarrow \mu\rho^0$ mode, the dominant background comes from $e^+e^- \rightarrow q\bar{q}$ events. A smaller background of generic $\tau^+\tau^-$ events in the region $\Delta E < 0 \text{ GeV}$ and $M_{\mu V^0} < m_\tau$ is due to combinations

TABLE II: Summary of $M_{\ell V^0}$ and ΔE resolutions ($\sigma_{M_{\ell V^0}}^{\text{high/low}}$ (MeV/ c^2) and $\sigma_{\Delta E}^{\text{high/low}}$ (MeV)). Here σ^{high} (σ^{low}) means the standard deviation on the higher (lower) side of the peak.

Mode	$\sigma_{M_{\ell V^0}}^{\text{high}}$	$\sigma_{M_{\ell V^0}}^{\text{low}}$	$\sigma_{\Delta E}^{\text{high}}$	$\sigma_{\Delta E}^{\text{low}}$
$\tau \rightarrow \mu \rho^0$	6.1	5.4	16.0	21.9
$\tau \rightarrow e \rho^0$	6.7	5.7	15.6	25.1
$\tau \rightarrow \mu \phi$	3.7	3.8	14.2	19.9
$\tau \rightarrow e \phi$	4.1	4.5	14.0	22.0
$\tau \rightarrow \mu \omega$	7.0	8.9	25.7	29.0
$\tau \rightarrow e \omega$	8.6	9.7	21.1	37.1
$\tau \rightarrow \mu K^{*0}$	4.9	5.2	15.8	21.2
$\tau \rightarrow e K^{*0}$	5.7	6.7	15.6	25.1
$\tau \rightarrow \mu \bar{K}^{*0}$	4.9	5.2	15.8	21.3
$\tau \rightarrow e \bar{K}^{*0}$	5.2	5.7	15.6	24.6

of a fake muon and two pions. For the $\tau \rightarrow \mu \omega$ mode, there is a small background in the signal region from generic $\tau^+ \tau^-$ events in which a fake muon is combined with two pions from $\tau^- \rightarrow \pi^- \pi^+ \pi^- \nu_\tau$ and a fake π^0 (from ISR and beam background). A large background is from $\tau^- \rightarrow h^- \omega \nu_\tau$ in the $\Delta E < 0$ GeV and $M_{\mu V^0} < m_\tau$ region. For the $\tau \rightarrow \mu \phi$ mode, the dominant background is due to $q\bar{q}$ and $\tau^+ \tau^-$ events in which a pion is misidentified as a kaon. For the $\tau \rightarrow \mu K^{*0}$ and $\mu \bar{K}^{*0}$ modes, the dominant background comes from generic $\tau^+ \tau^-$ events with a fake muon, fake kaon and real pion from $\tau^- \rightarrow \pi^- \pi^+ \pi^- \nu_\tau$. If one of the pions is misidentified as a kaon, then the reconstructed mass from generic $\tau^+ \tau^-$ background could be greater than the τ lepton mass, since the kaon mass is greater than that of the pion.

For the $\mu \rho^0$ and $\mu \omega$ modes, where significant background remains after applying the above-mentioned selection criteria, we extrapolate to the signal region by fitting to observed data in the $\pm 5\sigma_{\Delta E}$ $M_{\mu V^0}$ data sideband using the sum of an exponential and a first-order polynomial function for generic $\tau^+ \tau^-$ and continuum, respectively. For the $\tau \rightarrow e V^0$, $\mu \phi$, μK^{*0} and $\mu \bar{K}^{*0}$ modes, the background after all the event selection requirements have been applied is small; extrapolation to the signal region assumes that the background distribution is flat along the $M_{\ell V^0}$ axis within $\pm 5\sigma_{\Delta E}$. We estimate the expected number of the background events in the signal region for each mode using the number of data events observed in the sideband region inside the horizontal lines but outside the signal region. The signal efficiency and background level for each mode are given in Table III. After estimating the background, we open the blinded regions. We observe one candidate event for each of the $\tau \rightarrow \mu \phi$, μK^{*0} and $\mu \bar{K}^{*0}$ modes, and no candidate events for other modes. In each case the number of events observed in the signal region is consistent with the expected number of background events.

The dominant systematic uncertainties in this analysis relate to tracking efficiencies and particle identification. The uncertainty due to the track finding efficiency is estimated to be 1.0% per charged track, therefore, the total uncertainty due to the charged track finding is 4.0%. The uncertainty due to particle identification is 2.2%, 1.9%, 1.3% and 1.8% per electron, muon, pion and kaon, respectively. The uncertainties due to the V^0 branching

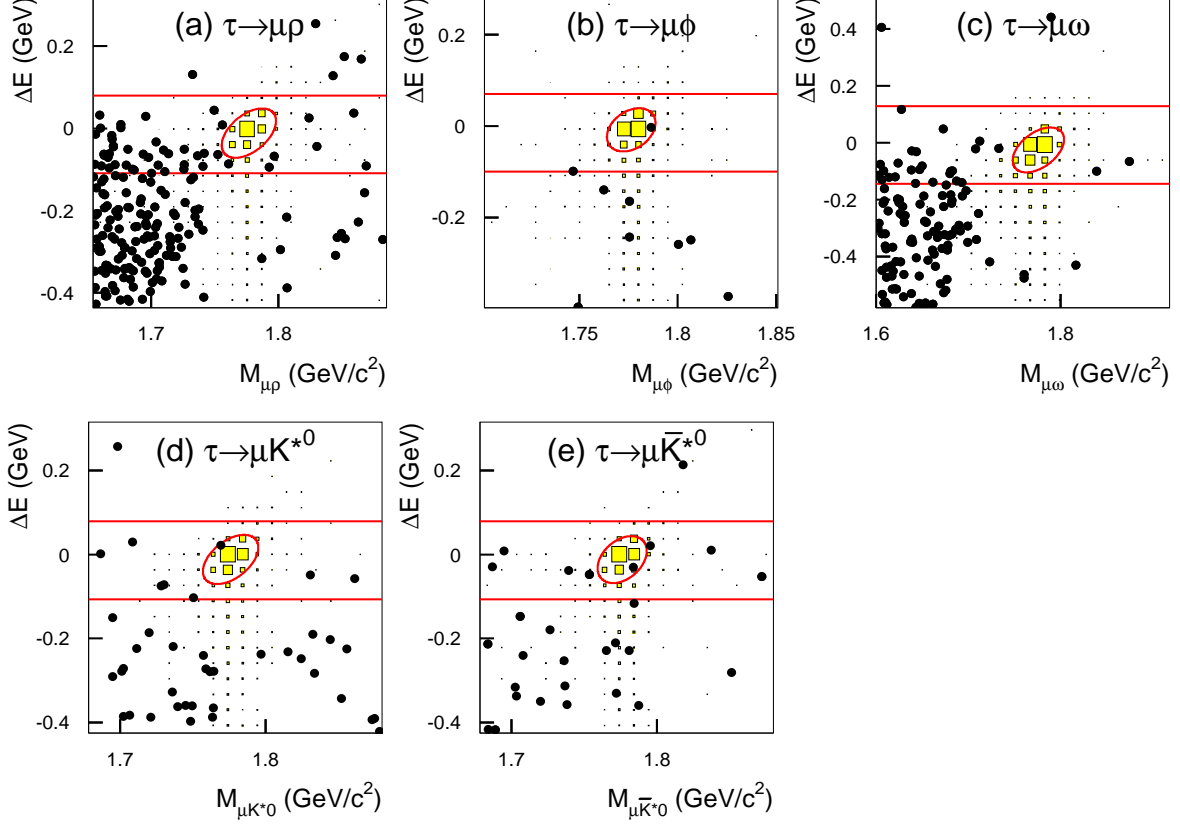


FIG. 4: Scatter-plots in the $\pm 20\sigma$ area of the $M_{\mu V^0} - \Delta E$ plane: (a), (b), (c), (d) and (e) show the $\mu\rho^0$, $\mu\phi$, $\mu\omega$, μK^{*0} and $\mu\bar{K}^{*0}$ modes, respectively. Experimental data events are shown as solid circles. The filled boxes show the MC signal distributions with arbitrary normalization. The elliptical signal (blind) regions shown by solid curves are used for evaluating the signal yield. The region between the horizontal solid lines (excluding the signal region) is used to estimate the expected background in the elliptical region.

fractions are estimated to be 1.2% and 0.7% for the ϕ and ω , respectively. The uncertainty due to the integrated luminosity is estimated to be 1.4%. The uncertainties due to the trigger efficiency and MC statistics are negligible compared with the other uncertainties. All these uncertainties are added in quadrature, and the total systematic uncertainties for the different modes range from 5.3% to 6.2%, as shown in Table III.

UPPER LIMITS ON THE BRANCHING FRACTIONS

Since no statistically significant excess of data over the expected background is observed in the signal region, we set upper limits on the branching fractions based on a frequentist approach [21]. We calculate the 90% C.L. upper limit on the number of signal events including systematic uncertainty (s_{90}) from the number of expected background events, the number of observed events and the systematic uncertainty, using the POLE program without

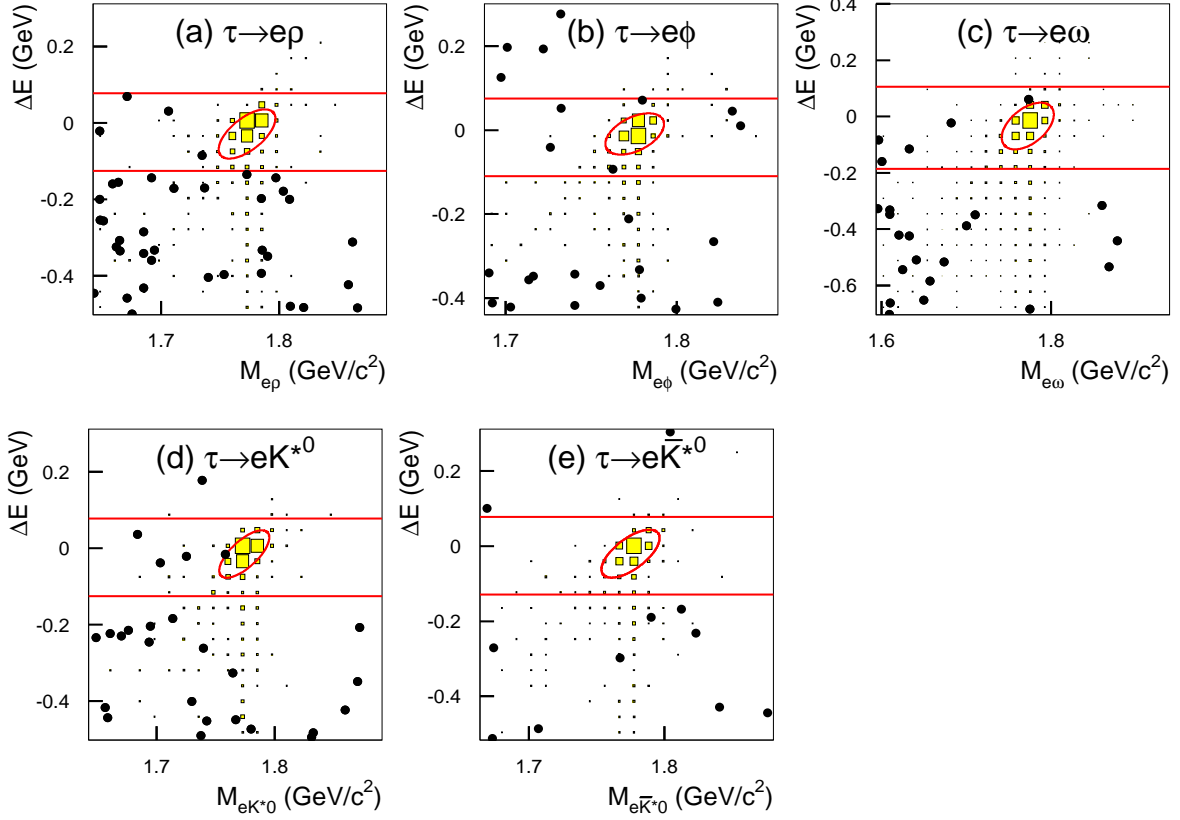


FIG. 5: Scatter-plots in the $\pm 20\sigma$ area of the $M_{eV^0} - \Delta E$ plane: (a), (b), (c), (d) and (e) show the $e\rho^0$, $e\phi$, $e\omega$, eK^{*0} and $e\bar{K}^{*0}$ modes, respectively. Experimental data events are shown as solid circles. The filled boxes show the MC signal distributions with arbitrary normalization. The elliptical signal (blind) regions shown by solid curves are used for evaluating the signal yield. The region between the horizontal solid lines (excluding the signal region) is used to estimate the expected background in the elliptical region.

conditioning [22]. The upper limit on the branching fraction (\mathcal{B}) is then given by

$$\mathcal{B}(\tau \rightarrow \ell V^0) < \frac{s_{90}}{2N_{\tau\tau}\varepsilon}, \quad (1)$$

where $N_{\tau\tau}$ is the number of $\tau^+\tau^-$ pairs, and ε is the signal efficiency including the branching fraction of V^0 . The value $N_{\tau\tau} = 782 \times 10^6$ is obtained from the integrated luminosity times the cross section of τ -pair production, which is calculated in KKMC [23] to be $\sigma_{\tau\tau} = 0.919 \pm 0.003$ nb and $\sigma_{\tau\tau} = 0.875 \pm 0.003$ nb for 782 fb^{-1} at $\Upsilon(4S)$ and 72 fb^{-1} at $\Upsilon(5S)$, respectively. Table III summarizes information about upper limits for all modes. We obtain the following ranges for 90% C.L. upper limits on the branching fractions: $\mathcal{B}(\tau \rightarrow eV^0) < (1.8 - 4.8) \times 10^{-8}$ and $\mathcal{B}(\tau \rightarrow \mu V^0) < (1.2 - 8.4) \times 10^{-8}$. These results improve upon our previously published upper limits [10] by factors of up to 5.7. They are also more restrictive than the recent results from BaBar [11, 12].

TABLE III: The signal efficiency (ε), the number of expected background events (N_{BG}) estimated from the sideband data, total systematic uncertainty (σ_{syst}), the number of observed events in the signal region (N_{obs}), 90% C.L. upper limit on the number of signal events including systematic uncertainties (s_{90}), 90% C.L. upper limit on the observed branching fraction ($\mathcal{B}_{\text{obs.}}$) for each individual mode.

Mode	ε (%)	N_{BG}	σ_{syst} (%)	N_{obs}	s_{90}	$\mathcal{B}_{\text{obs}} (\times 10^{-8})$
$\tau^- \rightarrow \mu^- \rho^0$	7.09	1.48 ± 0.35	5.3	0	1.34	1.2
$\tau^- \rightarrow e^- \rho^0$	7.58	0.29 ± 0.15	5.4	0	2.17	1.8
$\tau^- \rightarrow \mu^- \phi$	3.21	0.06 ± 0.06	5.8	1	4.24	8.4
$\tau^- \rightarrow e^- \phi$	4.18	0.47 ± 0.19	5.9	0	2.02	3.1
$\tau^- \rightarrow \mu^- \omega$	2.38	0.72 ± 0.18	6.1	0	1.76	4.7
$\tau^- \rightarrow e^- \omega$	2.92	0.30 ± 0.14	6.2	0	2.19	4.8
$\tau^- \rightarrow \mu^- K^{*0}$	3.39	0.53 ± 0.20	5.5	1	3.81	7.2
$\tau^- \rightarrow e^- K^{*0}$	4.37	0.29 ± 0.14	5.6	0	2.17	3.2
$\tau^- \rightarrow \mu^- \bar{K}^{*0}$	3.60	0.45 ± 0.17	5.5	1	3.90	7.0
$\tau^- \rightarrow e^- \bar{K}^{*0}$	4.41	0.08 ± 0.08	5.6	0	2.34	3.4

SUMMARY

We have searched for lepton-flavor-violating τ decays into a lepton and a vector meson using 854 fb^{-1} of data collected with the Belle detector at the KEKB asymmetric-energy e^+e^- collider. Since no evidence for a signal is found, we set the following 90% C.L. upper limits on the branching fractions: $\mathcal{B}(\tau \rightarrow eV^0) < (1.8 - 4.8) \times 10^{-8}$ and $\mathcal{B}(\tau \rightarrow \mu V^0) < (1.2 - 8.4) \times 10^{-8}$. These results improve upon our previously published upper limits by factors of up to 5.7. This improvement results both from using a larger data sample and from an improved rejection of specific backgrounds, such as di-baryon production in the continuum for the $\tau \rightarrow \mu V^0$ modes, and $\tau^- \rightarrow h^- \pi^0 \nu_\tau$ decays with a photon conversion for the $\tau \rightarrow eV^0$ modes. The more stringent upper limits reported here can be used to constrain the parameter space in various models of new physics.

Acknowledgments

We thank the KEKB group for the excellent operation of the accelerator, the KEK cryogenics group for the efficient operation of the solenoid, and the KEK computer group and the National Institute of Informatics for valuable computing and SINET3 network support. We acknowledge support from the Ministry of Education, Culture, Sports, Science, and Technology (MEXT) of Japan, the Japan Society for the Promotion of Science (JSPS), and the Tau-Lepton Physics Research Center of Nagoya University; the Australian Research Council and the Australian Department of Industry, Innovation, Science and Research; the National Natural Science Foundation of China under contract No. 10575109, 10775142, 10875115 and 10825524; the Ministry of Education, Youth and Sports of the Czech Republic under contract No. LA10033 and MSM0021620859; the Department of Science and Technology of India; the BK21 and WCU program of the Ministry Education Science and Technology,

National Research Foundation of Korea, and NSDC of the Korea Institute of Science and Technology Information; the Polish Ministry of Science and Higher Education; the Ministry of Education and Science of the Russian Federation and the Russian Federal Agency for Atomic Energy; the Slovenian Research Agency; the Swiss National Science Foundation; the National Science Council and the Ministry of Education of Taiwan; and the U.S. Department of Energy. This work is supported by a Grant-in-Aid from MEXT for Science Research in a Priority Area (“New Development of Flavor Physics”), and from JSPS for Creative Scientific Research (“Evolution of Tau-lepton Physics”).

-
- [1] J. E. Kim, P. Ko and D. G. Lee, Phys. Rev. D **56**, 100 (1997).
 - [2] A. Ilakovac, Phys. Rev. D **62**, 036010 (2000).
 - [3] D. Black *et al.*, Phys. Rev. D **66**, 053002 (2002).
 - [4] C.-H. Chen and C.-Q. Geng, Phys. Rev. D **74**, 035010 (2006).
 - [5] E. Arganda *et al.*, JHEP **0806**, 079 (2008).
 - [6] R. Benbrik and C. H. Chen, Phys. Lett. B **672**, 172 (2009).
 - [7] Z. H. Li, Y. Li and H. X. Xu, Phys. Lett. B **677**, 150 (2009).
 - [8] A. Abashian *et al.* (Belle Collaboration), Nucl. Instr. and Meth. A **479**, 117 (2002).
 - [9] S. Kurokawa and E. Kikutani, Nucl. Instr. and Meth. A **499**, 1 (2003), and other papers included in this Volume.
 - [10] Y. Nishio *et al.* (Belle Collaboration), Phys. Lett. B **664**, 35 (2008).
 - [11] B. Aubert *et al.* (BaBar Collaboration), Phys. Rev. Lett. **103**, 021801 (2009).
 - [12] B. Aubert *et al.* (BaBar Collaboration), Phys. Rev. Lett. **100**, 071802 (2008).
 - [13] K. Hanagaki *et al.*, Nucl. Instr. and Meth. A **485**, 490 (2002).
 - [14] A. Abashian *et al.*, Nucl. Instr. and Meth. A **491**, 69 (2002).
 - [15] S. Jadach *et al.*, Comp. Phys. Commun. **130**, 260 (2000).
 - [16] D. J. Lange, Nucl. Instr. and Meth. A **462**, 152 (2001).
 - [17] S. Jadach *et al.*, Comp. Phys. Commun. **70**, 305 (1992).
 - [18] F. A. Berends *et al.*, Comp. Phys. Commun. **40**, 285 (1986).
 - [19] S. Brandt *et al.*, Phys. Lett. **12**, 57 (1964); E. Farhi, Phys. Rev. Lett. **39**, 1587 (1977).
 - [20] K. Hayasaka *et al.* (Belle Collaboration), Phys. Lett. B **613**, 20 (2005).
 - [21] G. J. Feldman and R. D. Cousins, Phys. Rev. D **57**, 3873 (1998).
 - [22] See <http://www3.tsl.uu.se/~conrad/pole.html>; J. Conrad *et al.*, Phys. Rev. D **67**, 012002 (2003).
 - [23] S. Banerjee *et al.*, Phys. Rev. D **77**, 054012 (2008).